CSCanada
Advances in Natural Science
Vol. 6, No. 4, 2013, pp. 1-14
DOI:10.3968/j.ans.1715787020130604.2838

ISSN 1715-7862 [PRINT]
ISSN 1715-7870 [ONLINE]
www.cscanada.net
www.cscanada.org

Neuralized Mouse Embryonic Stem Cells Develop Neural Rosette-Like Structures in Response to Retinoic Acid and Produce Teratomas in the Brains of Syngeneic Mice

Cheryl L. Dunham[a]; Mark D. Kirk[a],*

[a]Division of Biological Sciences, University of Missouri, Columbia, MO, USA.
*Corresponding Author.

Received 30 August 2013; accepted 11 November 2013

Abstract

Several induction protocols can direct differentiation of mouse embryonic stem cells (ESCs) to become neural cells. The B5 and B6 mouse ESC lines display different growth patterns in vitro, and when grown as adherent cultures, the B6 ESCs proliferated at a significantly lower rate than B5 ESCs. Remarkably, after a neural induction protocol that includes removal of LIF and addition of retinoic acid (RA), mature B6 embryoid bodies (EBs) displayed a unique neural rosette-like morphology. On Day 8 of neural induction, B6 EBs revealed mature neuronal markers localized primarily to cells in the center of the EBs and glial markers expressed both in centrally and peripherally located cells. In contrast to B5 cells, when neuralized Day 8 B6 EB cells were dissociated and transplanted into the left striatum of syngeneic C57BL/6 mouse brains, teratomas formed. In addition, teratomas established from undifferentiated B6 cells grew more rapidly and achieved larger volumes when compared to those produced by Day 8, neuralized B6 EBs. The slow growth rate of B6 cells *in vitro* may have contributed to incomplete neuralization, formation of neural rosette-like structures, and a propensity to form teratomas.

Key words: C57BL/6 mouse; Embryoid bodies; Embryonic stem cells; Neural stem cells; Neural induction; Striatum; Teratoma

Cheryl L. Dunham, Mark D. Kirk (2013). Neuralized Mouse Embryonic Stem Cells Develop Neural Rosette-Like Structures in Response to Retinoic Acid and Produce Teratomas in the Brains of Syngeneic Mice. *Advances in Natural Science*, *6*(4), 1-14. Available from: http://www.cscanada.net/index.php/ans/article/view/j.ans.1715787020130604.2838
DOI: http://dx.doi.org/10.3968/j.ans.1715787020130604.2838

INTRODUCTION

Stem cells are classified in part by their ability to produce various types of specialized cells (Eisenberg & Eisenberg, 2003). Pluripotent stem cells can differentiate into cells of all three primary embryonic germ layers, ectoderm, mesoderm, and endoderm and can contribute to germ line transmission. Embryonic stem cells (ESCs) are pluripotent and are found in the inner cell mass of the blastocyst (Eisenberg & Eisenberg, 2003; Mitalipov & Wolf, 2009; Solter, 2006; Alison & Islam, 2009).

Due to their broad potential for differentiation, pluripotent stem cells are of particular importance in the fields of developmental biology and regenerative medicine. Before ESC lines were established, pluripotent cell lines were obtained from teratocarcinomas, tumors that can produce tissue types representative of all three primary embryonic germ layers (Solter, 2006; Li & Tanaka, 2011; Kleinsmith & Pierce, 1964). In early studies, the 129SvJ mouse strain was found to have a 1% spontaneous rate of occurrence of testicular teratomas (Solter, 2006; Stevens & Little, 1954). Cells from some of these teratomas could be extracted, cultured, and injected subcutaneously into syngeneic recipients to produce additional teratomas or injected intraperitoneally to form aggregates that were organized in a manner that resembled embryos, and were therefore called embryoid bodies (EBs) (Kleinsmith & Pierce, 1964). Teratoma formation has become a standard by which to assess stem cell plasticity and is still used as a measure of pluripotency (Okita, Ichisaka, & Yamanaka, 2007). Teratomas are frequently assessed via histological staining and by immunocytochemical detection of markers for tissues derived from the primary embryonic germ layers (Li & Tanaka, 2011; Shao et al., 2007; Takahashi et al., 2007; Takahashi & Yamanaka, 2006; Martin, 1981).

An area of special interest for ESC-based cell therapies is treatment of neurodegenerative disorders. Diseases of the central nervous system (CNS), such as amyotrophic lateral sclerosis and Parkinson's disease, are debilitating and currently have no cure; however, stem cell therapies could replace nerve cells lost due to the pathology and restore neurological function (Srivastava, Malhotra, Sharp, & Berggren, 2008). Many induction protocols for ESCs have been developed that produce a variety of neural progeny including cholinergic, dopaminergic, serotonergic, GABAergic, and glutamatergic neurons, as well as glial cells, including oligodendrocytes and astrocytes (Cai & Grabel, 2007; Bibel et al., 2004; Wang et al., 2009; Bjorklund et al., 2002; Lee, Lumelsky, Studer, Auerbach, & McKay, 2000; Meyer, Katz, Maruniak, & Kirk, 2004; Okabe, Forsberg-Nilsson, Spiro, Segal, & McKay, 1996; Bain, Kitchens, Yao, Huettner, & Gottlieb, 1995).

Genetic, morphological, behavioral, and neuroanatomical variability exists between members of different mouse strains and even among substrains of specific murine lineages (Bryant et al., 2008; Chen et al., 2006; Crusio, Schwegler, & Van Abeelen, 1991; Auerbach et al., 2000; Kawase et al., 1994; Tabibnia, Cooke, & Breedlove, 1999; Wahlsten, Metten, & Crabbe, 2003; Ledermann, 2000; Cook, Bolivar, McFadyen, & Flaherty, 2002), and based on these differences, one would predict differences in ESC lines derived from different mouse strains. Many transgenic mouse models are derived from the C57BL/6 mouse strain, and it would be advantageous to use C57BL/6-derived ESC cell lines, such as the B6 ESC cell line, for transplantation experiments (Kawase et al., 1994; Ledermann & Burki, 1991; Gertsenstein et al., 2010; Hughes et al., 2007). However, previous studies show that C57BL/6-derived ESCs can exhibit slower growth rates when compared to 129/SvJ-derived ESCs, thus leading to lower efficiency rates in establishing chimeras and knockout mice (Auerbach et al., 2000; Kawase et al., 1994; Ledermann & Burki, 1991; Gertsenstein et al., 2010; Cheng, Dutra, Takesono, Garrett-Beal, & Schwartzberg, 2004; Brook & Gardner, 1997; Seong, Saunders, Stewart, & Burmeister, 2004; Collins, Rossant, & Wurst, 2007; Ware, Siverts, Nelson, Morton, & Ladiges, 2003; Keskintepe, Norris, Pacholczyk, Dederscheck, & Eroglu, 2007).

To assess the potentials of different ESC lines for brain transplantation, in the current study we performed a comparative analysis of the ESC lines B5 (129/SvJ-derived) and B6 (C57BL/6-derived). The current analysis included tests of their growth responses in culture, their *in vitro* response to the 4–/4+ retinoic acid neural induction protocol (Bain et al., 1995), and their ability to form teratomas *in vivo* after implantation into the brains of mature mice.

1. MATERIALS AND METHODS

1.1 Cell Culture

Mouse ESCs were cultured according to protocols described previously (Bain et al., 1995; Meyer, Katz, Maruniak, & Kirk, 2006). Briefly, enhanced green fluorescent protein (EGFP) expressing mouse B6 ESCs [C57BL/6J-Tg (ActinB:EGFP) OsbY01], obtained from the Murine Embryonic Stem Cell Core (Washington University, St. Louis) and B5 mouse ESCs (S129) (Meyer et al., 2004; Meyer et al., 2006; Pierret et al., 2007; Pierret et al., 2010), obtained from Dr. Andras Nagy, Samuel Lunenfeld Research Institute (Mt. Sinai Hospital, Toronto, Ontario, Canada) were cultured on feeder-free, gelatin-coated T25 flasks (Midwest Scientific, Catalog number: TP90025) containing 5 mL ESC growth medium (ESGM) and 1000 U/mL leukemia inhibitory factor (LIF; Millipore, Catalog number: ESG1106). ESGM contained Dulbecco's modified Eagle medium (DMEM; Gibco, Catalog number: 11965-092), 10% newborn calf serum, 10% fetal bovine serum, 5% nucleoside stock (consisting of 0.80 mg/mL adenosine, 0.85 mg/mL guanosine, 0.73 mg/mL cytidine, 0.73 mg/mL uridine, and 0.24 mg/mL thymidine), and 1 mM β-mercaptoethanol (βME). After growth to approximately 70% confluence, cells were exposed to 0.25% trypsin, mechanically dissociated, and passaged to new T25 flasks at a ratio of 1:2 or 1:3. The newly plated cells were checked using phase contrast microscopy to ensure that a majority existed as single cells in suspension.

The 4–/4+ protocol of Bain et al. (1995) was used to induce ESCs to a neural fate. To achieve this neural induction, colonies were grown to 70% confluence, dissociated as described above, passed through a 40 microns cell strainer and transferred to uncoated petri dishes containing ESC induction media (ESIM) for 4 days. ESIM consisted of the same components as ESGM, but lacked LIF and βME. The cells established spherical aggregates (i.e., EBs). After four days, the EBs were then cultured for an additional four days in ESIM containing 500 nM all-*trans* retinoic acid (RA; Sigma-Aldrich, Catalog number: R2625), a potent neuralizing agent (Cheng et al., 2004; Faherty, Kane, & Quinlan, 2005; Yamanaka et al., 2008). Prior to transplantation on Day 8 of induction, the neuralized EBs were treated with 0.25% trypsin for 8 minutes and dissociated mechanically using repeated pipetting. Cell counts were performed using a hemocytometer, and trypan blue exclusion was used as a measure of cell viability.

1.2 Transplantations

Because both the B5 and B6 ESC lines were derived from male mouse strains, male mice were used for all transplant experiments to enhance immune compatibility. Mature C57BL/6 mice were anesthetized using mouse anesthetic

cocktail [25 mg/mL Ketamine, 25 mg/mL LA Xylazine, and 0.5 mg/mL Acepromazine in 0.1M phosphate-buffered saline (PBS); 0.1 cc per 25 gm body weight, given IM]. Anesthetized mice were placed in a stereotactic device, and an incision was made anteroposteriorly across the midline of the head. An electric drill and bit were used to make a burr hole in the cranium large enough in diameter to accommodate a 36 gauge needle while targeting the left striatum using the following coordinates: anteroposterior -0.72 mm from bregma; lateromedial -1.73 mm from midline; dorsoventral -2.00 mm from skull. A 10 µL Hamilton syringe with a 36 gauge needle was inserted 3 mm below the surface of the cerebrum and then retracted 1 mm. This method targeted the left striatum and created a space for the implanted cells during injection. Undifferentiated or induced ESCs were dissociated as described above and re-suspended at 500,000 cells per microliter in DMEM. Two microliters of cell suspension was injected for a total of 1 million implanted cells. Vetbond™ tissue adhesive was used to close the skin incision.

Mice were euthanized 3 or 6 weeks after transplantation, depending on the experimental design. In all cases, anesthetized mice were perfused transcardially with 0.1M PBS followed by 4% phosphate-buffered paraformaldehyde (PFA). A volume of 30 mL of ice-cold PBS followed by 30 mL of ice-cold PFA were administered transcardially to each animal using a polystatic pump (Buchler Instruments) over a period of 12 minutes. Brains were removed and postfixed whole with 4% PFA for 36 hours and sucrose-protected by serial transfer into 10%, 20% and 30% sucrose in 0.17M sodium cacodylate buffer. Subsequently, brains were embedded in OCT and frozen at -20 °C. All animal care and treatment protocols followed MU Office of Animal Research guidelines and were approved by the MU Animal Care and Use Committee.

1.3 Immunohistochemistry

Embryoid bodies on Day 4 or Day 8 of neural induction (see above), were pelleted gently, fixed overnight at 4 °C in 4% PFA in 0.1 M PBS, equilibrated in 20% sucrose in 0.17 M sodium cacodylate, embedded in OCT, and frozen at -20 °C. Serial frozen sections of EBs and of host brains were cut with a Leica Cryostat (Molecular Cytology Core, University of Missouri-Columbia) at a thickness of 10 µm, mounted on SuperFrost™ Plus slides (Fisher, Catalog number: 12-550-15), immersed in 0.1 M PBS, and placed on a rocker at low speed for 15 minutes. Sections were then permeabilized and blocked using 0.3% Triton X-100 in 0.1 M PBS and 10% normal goat serum (NGS) for one hour at room temperature. Primary antibodies selective for pluripotent stem cells (mouse monoclonal for OCT3/4, also designated POU5F1, 1:250, Santa Cruz, Catalog number: sc-5279), neural precursors [mouse monoclonal for nestin (NES), 1:200, Millipore, Catalog number: MAB353], immature neurons [mouse monoclonal for β-III Tubulin (TUBB3), 1:100, Promega, Catalog number: G7121], astrocytes [rabbit polyclonal for glial fibrillary acidic protein (GFAP), 1:1000, Dako, Catalog number: z0334], mature neurons [rabbit polyclonal for Neurofilament-M (NF-M), 1:200, Millipore, Catalog number: AB1987], mesoderm [rabbit polyclonal for Brachyury (BRY), 1:100, Abcam, Catalog number: ab2068], and endoderm [mouse monoclonal for α-fetoprotein (AFP), 1:100, Cell Signaling, Catalog number: 3903S] were diluted in 0.1 M PBS containing 2% NGS and 0.5% Triton X-100 and applied to sections overnight at 4 °C. Samples were then washed 5 times with 0.1 M PBS at 5 minute intervals. Appropriate fluorescent-tagged goat anti-mouse (Alexa Fluor® 546, Molecular Probes, Catalog number: A11003) or goat anti-rabbit (Alexa Fluor® 546, Molecular Probes, Catalog number: A11010) antibodies were diluted 1:200 in 0.1 M PBS containing 2% NGS, 0.5% Triton X-100, and the nuclear stain, DAPI (1:300, Molecular Probes, Catalog number: D3571) and applied for 1-4 hours at room temperature. Controls were performed in parallel with each treatment group and were processed using the above protocol, without the primary antibody. After application of the secondary antibody, samples were washed 8 times at 5 minute intervals with 0.1 M PBS. Coverslips were applied using a Mowiol solution [0.1 M TRIS at pH 8.5, 10% MOWIOL® Reagent 4-88 (Calbiochem, Catalog number: 47904), 25% glycerol]. Brain sections were imaged using a Leica M205 FA stereomicroscope with a Leica DFC 345 FX camera and processed using LAS AF Lite version 2.4.1, build 6384 and ImageJ version 1.43. Mounted sections of EBs were imaged using an Olympus IX70 inverted microscope equipped with a Hamamatsu ORCA-AG deep-cooled CCD camera, and 8-bit TIF images were processed using MetaMorph version 6.3r6 and ImageJ version 1.43. Images of immunolabeled samples were captured and processed at the Molecular Cytology Core, University of Missouri-Columbia.

1.4 Measurements and Statistics

1.4.1 Embryonic Stem Cell Colonies and Embryoid Bodies

Images of adherent ESC cultures were captured using an inverted Olympus IX70 microscope equipped with a Photometric Sensys CCD camera OpenLab 2.2.5 software (Improvision). Colony diameters were measured using ImageJ software, version 1.43. Two days after passage, a minimum of six colonies were chosen randomly (using a coordinate grid and random numbers generated by Microsoft Excel) from a minimum of three different preparations for each treatment group (i.e., B6 colonies passaged at a ratio of 1:2, B6 colonies passaged at a ratio of 1:3, and B5 colonies passaged at a ratio of 1:3) and

mean colony diameters and standard deviations were calculated. Random image samples and mean diameters for unlabeled EBs were obtained in a manner similar to that described above for ESC colonies, with mean EB diameters obtained from a minimum of five preparations.

Percentages for immunolabeling were determined for sectioned B6 EBs. Images of EB sections, obtained at the center of the EB spheres, were taken through an EGFP filter (all cells within the EBs express EGFP). Images of EGFP fluorescence were analyzed with ImageJ version 1.43 software to determine the cross-sectional areas of the EBs within the field of view. Images of identical regions were also taken with a Texas Red filter, used to reveal Alexa Fluor® 546 emissions from the secondary antibodies. The latter images were analyzed to determine the area within the EB sections that expressed a specific marker (see Immunohistochemistry). The percentages of EB areas labeled for a given marker were obtained by dividing the area expressing the marker by the area expressing EGFP (n = 5 for each antibody label). Comparisons of percentages of EBs with marker expression were analyzed within the Day 4 and the Day 8 EB treatment groups for all markers tested.

1.4.2 Quantification of Tumor Volume

Volumetric comparisons of tumors were made from serial frozen sections. To sample tumor volumes, images of sectioned brain tumors were taken every tenth section across the entire tumor. Sections were imaged through an EGFP filter using a Leica M205 FA Stereomicroscope with the Leica AF6000 software application. ImageJ version 1.43 was used to threshold and select EGFP-expressing tissue and to measure section area (A_n) containing donor cells and their progeny. Area measurements were converted to sampled tumor volume (V_S) by summing the product of section area and section thickness ($10\ \mu m$) for all tumor sections analyzed, using the following formula:

$$V_S = \Sigma\ (A_n \times 10\ \mu m)$$

1.4.3 Statistical Analyses

Data were analyzed using OriginPro 8 SR0 software, version 8.0724. Pairwise comparisons were made using a t-test assuming a two-tailed sample distribution and unequal variance was used for all statistical tests ($p < 0.001$). Comparisons of three or more treatment groups were made using a one-way analysis of variance (ANOVA) and a Scheffé post hoc test. The significance levels for ANOVA and Scheffé post hoc tests were set at $p < 0.01$.

2. RESULTS

2.1 Characterization of B5 & B6 ESCs in Vitro and of Neural Rosette-Like Formations

Murine B5 and B6 embryonic stem cells were passed from one T25 flask to three T25 flasks (a ratio of 1:3). After 2 days of growth as attached cell cultures containing LIF, B6 ESCs produced small circular colonies. However, many of the B6 colonies were irregularly shaped and often lacked the sharply defined edges characteristic of colonies produced by S129-derived, B5 ESCs (Figure 1A, B; Keskintepe, et al., 2007; Limaye, et al., 2009). B6 ESC colonies passaged at a ratio of 1:3 averaged 130 ± 10 µm in diameter and were significantly smaller than B5 ESC cell colony diameters passaged at 1:3 ($p < 0.0001$). The latter averaged 450 ± 60 µm in diameter (Figure 2A).

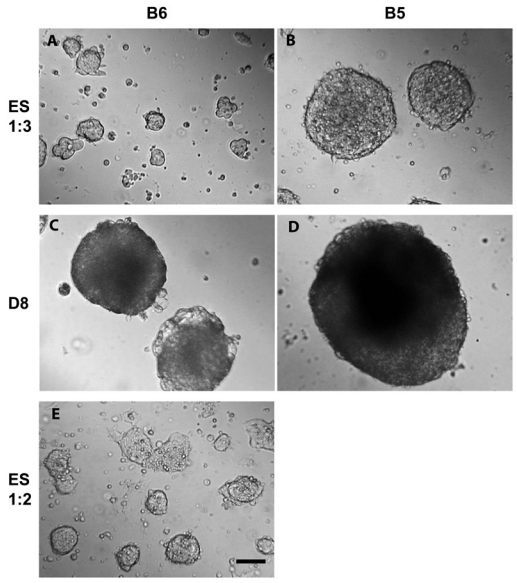

Figure 1
Embryonic Stem Cells (ESCs) **Derived From the Mouse Strain C57BL/6J-EGFP** (B6) **Grow More Slowly and Form Less Compact Colonies When Compared to ESC Colonies Derived From the 129svj** (B5) **Mouse Strain**

(A-B) Morphologies of B5 and B6 ESC colonies two days after passaging cells at a ratio of 1:3 from 70% confluent T-25 flasks. B5 ESCs form larger colonies with well-defined edges, compared to colonies formed by B6 ESCs. **(C-D)** Morphology of representative B5 and B6 embryoid bodies (EBs) following the neural induction protocol. Neurally-induced B6 EBs were smaller in diameter than B5 EBs. **(E)** Morphology of B6 ESC colonies two days after passaging cells at 70% confluency into T-25 flasks at a ratio of 1:2. Note that these cell colonies are larger than B6 ESC colonies passaged at a ratio of 1:3, showing the positive correlation between cell density and colony growth. Scale bar in E is 200 µm and applies to all panels.

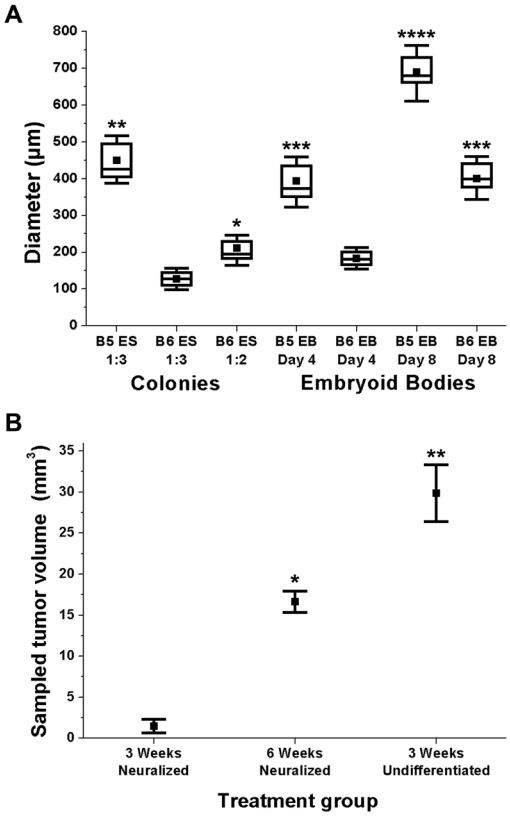

Figure 2
Growth and Colony Characteristics of B5 and B6 ESCs in Culture and After Transplantation Into Brains Of C57BL/6 Mice

(A) Comparisons of the diameters of B5 and B6 ESC colonies and B5 and B6 EBs at Day 4 and Day 8 of the neural induction protocol. B6 ESCs passaged at a ratio of 1:2 produced colonies with mean diameters significantly greater than those passaged at a ratio of 1:3 (*), and B5 ESCs passaged at a ratio of 1:3 produced colonies with mean diameters significantly greater than B6 colonies at all B6 passage ratios ($p < 0.001$). B5 EBs at Day 4 and B6 EBs at Day 8 had mean diameters that were significantly greater ($p < 0.001$) than those of B6 Day 4 EBs (***). Mean diameters of B5 Day 8 EBs were significantly greater ($p < 0.001$) than all other EBs grown in all other conditions tested (****). (B) After transplantation into the left striatum of syngeneic C57BL/6 mice, mean sampled tumor volume (V_s; see Materials and Methods) for undifferentiated B6 ESCs at 3 weeks post-transplantation was significantly greater ($p < 0.001$, **) than V_s produced by neuralized B6 ESCs at 3 weeks and 6 weeks post-transplantation. Also, 6 weeks after implantation of neuralized B6 ESCs, V_s was significantly greater ($p < 0.001$) than for implanted neuralized B6 ESCs at 3 weeks post-transplantation (*). For **(A)** and **(B)**, means are indicated by small filled squares (n = 4 for each condition) and error bars indicate standard deviations from the mean. In **(A)**, open boxes indicate the upper and lower 25% limits of the data range, and horizontal lines within these boxes show the medians.

To test whether increased initial cell plating density would improve B6 ESC colony properties (morphology and diameter), cells were grown to 70% confluency in T25 flasks and passaged at a ratio of 1:2. After a 1:2 passage and 2 days of growth, B6 ESC colony diameter was significantly increased ($p < 0.0001$, average diameter = 210 ± 30 µm) compared to cultures passaged at a ratio of 1:3 (Figures 1E, 2A). However, B6 ESC colony diameters were still significantly smaller than B5 ESC colonies passaged at a 1:3 ratio. Analysis of variance showed statistically significant ($p < 0.001$) differences among the mean colony diameters of the three treatment groups (B5 1:3 > B6 1:2 > B6 1:3).

Embryoid bodies were analyzed at Day 4 and Day 8 of neural induction. Embryoid bodies derived from B5 cells at Day 4 and from B6 cells at Day 8 had mean diameters that were significantly greater than those of Day 4 B6 EBs, with means of 390 ± 60 µm, 400 ± 60 µm, and 190 ± 20 µm respectively (Figure 2A). Embryoid bodies from B5 cells at Day 8 had mean diameters that were significantly greater than EBs grown in all other conditions tested ($p < 0.001$, B5 Day 8 average EB diameter = 690 ± 80 µm) (Figures 1C, D and 2A).

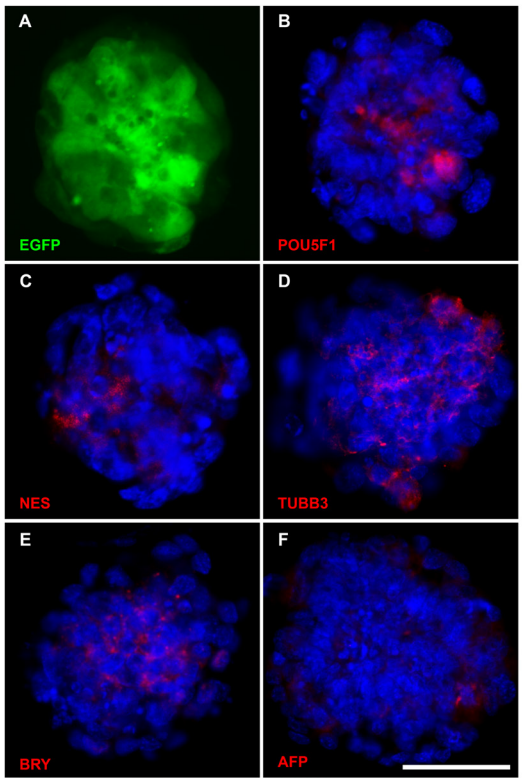

Figure 3
B6 Cells in Embryoid Bodies on Day 4 of the Neural Induction Protocol Express Markers for Pluripotent Stem Cells, Neural Precursors and Derivatives of the Three Primary Embryonic Germ Layers

(A) EBs express enhanced green fluorescent protein (EGFP). **(B-F)** B6 EBs express markers for a pluripotent stem cell transcription factor (POU5F1, **B**), neural precursors (NES, **C**), neuroectoderm (TUBB3, **D**), mesoderm (BRY, **E**), and endoderm (AFP, **F**). No labeling was observed in any EBs when the primary antibody was omitted (data not shown). Nuclei were stained with DAPI (blue). Immunolabeling was performed on 10 µm thick frozen sections. The scale bar in F is 50 µm and applies to all panels.

Table 1
Mean Percentages of Areas Labeled in B6 Embryoid Bodies for Specific Markers

EB Stage	Marker	Mean % Area (%) ± S. E.*
Day 4 embryoid bodies	α-fetoprotein	1.9 ± 0.3
	β-III tubulin	6.8 ± 0.6
	Brachyury	8.8 ± 0.5
	Nestin	8.8 ± 0.3
	POU5F1 (OCT3/4)	12.9 ± 0.4
Day 8 embryoid bodies	β-III tubulin	30.5 ± 1.6
	GFAP	16.1 ± 1.5
	Nestin	56.7 ± 0.6
	Neurofilament-M	15.0 ± 1.2

* Mean percentage area of embryoid bodies labeled was determined by the area labeled with specific markers divided by the area expressing EGFP and expressed as means ± Standard Errors (S.E.). Percentages are shown only for those markers tested where detectable amounts of expression were observed.

Prior to application of RA, Day 4 B6 EBs displayed markers for the three primary embryonic germ layers, ectoderm, mesoderm, and endoderm and for pluripotent stem cells (Figure 3). Immunolabeling of Day 4 B6 EBs revealed expression of POU domain class 5 transcription factor 1 (POU5F1), a pluripotency cell marker (Nichols et al., 1998) (also known as OCT3/4), in approximately 13% of the sampled cross-sectional areas (Figure 3B). The mean percentage of POU5F1 labeling for B6 Day 4 EBs was significantly greater than that of all other markers tested (Table 1). Slightly fewer cells were labeled for a neural precursor marker, nestin (Walker et al., 2010), the immature neuronal marker, β-III tubulin (Tubb 3) (Katsetos et al., 2001), and the early mesodermal marker, brachyury [Bry; Kispert & Herrmann, 1994] (Figure 3C, D, E; Table 1). Also, in Day 4 B6 EBs, some cells labeled for the early endodermal marker α-fetoprotein (Afp; Abe et al., 1996); the mean percentage of cells with NES, TUBB3 or BRY labeling was significantly greater than that for AFP (Figure 3F, Table 1).

After the application of RA starting on Day 4 of induction, EBs were induced towards a neural fate, with a greater percentage of cells expressing neural precursor, glial, and mature neuronal markers (Figure 4, Table 1). Immunolabeling of Day 8 B6 EBs revealed a high percentage of cross-sectional EB area expressing NES; in fact, the percentage of NES expression was significantly greater than that for all other markers tested ($p < 0.001$) (Figure 4A; Table 1). A large percentage of cells within the Day 8 EBs were labeled for the immature neuronal marker TUBB3, while less area was labeled for the astrocytic marker glial fibrillary acidic protein (GFAP) or the mature neuronal marker Neurofilament-M (NF-M; Figure 4B-D). There were significantly greater areas within the Day 8 B6 EBs labeled for NES or TUBB3 compared to that of Day 4 EBs ($p < 0.001$), and there was no detectable expression of GFAP or NF-M in Day 4 EBs. No labeling for AFP, BRY, or POU5F1 was found in Day 8 EBs. In Day 8 EBs, the percentage of TUBB3 expression was significantly greater than that for either GFAP or NF-M, while there were similar amounts of labeling for the latter two markers.

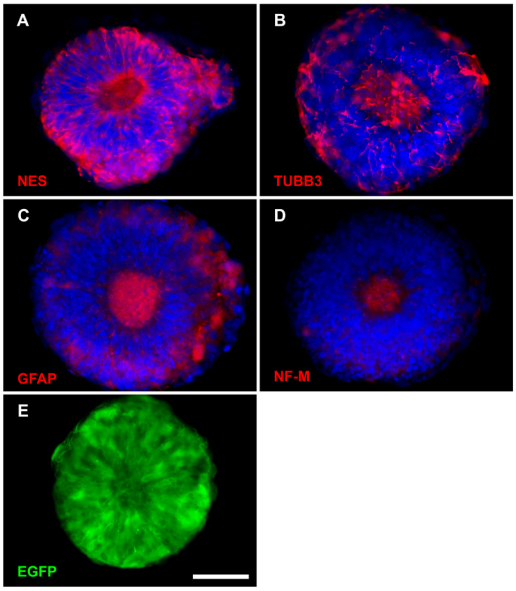

Figure 4
B6 Cells in Embryoid Bodies on Day 8 of Neural Induction Express Markers for Neural Precursors, Astrocytes, and Neurons, and the EBs Resemble Neural Rosettes

(A-D) Sections of Day 8 EBs exhibit markers for neural precursors (NES, **A**), immature neurons (TUBB3, **B**), astrocytes (GFAP, **C**), and mature neurons (NF-M, **D**). Note, in panels **B**, **C**, and **D** that a core of cells within the EBs exists that contains cells that label for TUBB3, GFAP, or NF-M, respectively. Although nestin was also expressed within the core, its expression was widely distributed throughout the EBs **(A)**. **E**, EGFP expression shows a rosette-like formation of cells. No expression of POU5F1, AFP, or BRY was observed in Day 8 B6 EBs. No labeling was observed in any EBs when the primary antibody was omitted. Nuclei were stained with DAPI (blue), and all images were taken from 10 µm thick frozen sections. The scale bar in **E** equals 100 µm and applies to all panels.

Cells within cross-sectioned Day 8 B6 EBs appeared to acquire the morphology similar to that of neural rosettes (Figure 4). These rosette-like structures consisted of a central spherical, cellular region of intact cells, surrounded by an annulus of cells. Although the central core of the EBs appeared to contain fewer cells than the surrounding periphery, the centrally located cells expressed markers for neural precursors, immature and mature neurons as well as astrocytes and possessed intact nuclei stained with DAPI (Figure 4). The neural markers were also expressed sparsely in peripheral regions of the EBs (Figure 4B, C, D). Nestin was expressed throughout the Day 8 B6

EBs, including NES expression in peripheral cells (Figure 4A). For Day 8 EBs that achieved a minimum diameter of 340 µm, a central core containing cells that expressed TUBB3, GFAP, and/or NF-M was observed in 95% of all B6 EBs analyzed (Figure 4; $n \geq 20$ sections). Results for marker expression in B5 EBs were similar to those described above, with the exception of the rosette-like structures, which were only observed in Day 8 B6 EBs (B5 data not shown; Meyer, et al., 2004).

2.2 Neuralized B6 ESCs Produce Teratomas in Syngeneic C57BL/6 Mouse Brain

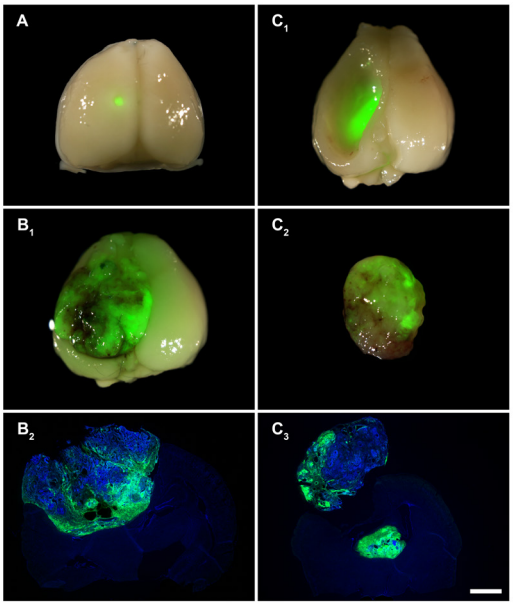

Figure 5
Examples of Brains Removed at 6 Weeks After Transplantation of EGFP Expressing, Neuralized B6 ESCs That Grew Teratomas in Syngeneic C57BL/6 Mice

(A-C) Tumors with portions that remained internal to the main brain parenchyma were seen in these samples. **(B-C)** In most cases, the tumor developed into a circumscribed mass. **(C_2)** In some cases, the tumor mass was easily isolated, such as this case where the tumor was removed from the sample shown in **C_1**. **B_2**, **C_3**, Coronal sections show the extent of tumor growth. Note the EGFP expression within tumor cells. Cellular nuclei were stained with DAPI, and images were taken from 10 µm thick frozen sections. The scale bar in **C3** equals 2 mm and applies to all panels.

In all cases (n = 8), both undifferentiated (data not shown) and neuralized B6 ESCs produced tumors when injected into the left striatum of mature, syngeneic C57BL/6 mice (Figure 5). The striatum was targeted because of its pivotal roles in certain neurological disorders that are targets for stem cell therapy, as well as to avoid penetrating the lateral ventricles. Tumor growth was extremely rapid in mice that received undifferentiated ESCs; consequently, all subjects receiving this treatment were sacrificed at 3 weeks post-transplantation, earlier than controls. As reported elsewhere (Spears, 2011) allogeneic transplants of B5 ESCs (129svj background), using the methods described here, were rejected within 2 weeks after implantation with no evidence of teratoma formation.

Transplanted neuralized cells were allowed to grow for 6 weeks, a period shown previously to be sufficient for induced ESCs to integrate into neural tissue (Meyer et al., 2004; Xu et al., 2005). The tumors displaced surrounding brain tissue and protruded into ventricular space (Figure 5). Tumors formed discrete masses and in some cases protruded beyond the dorsal brain surface. These circumscribed masses were distinct from surrounding brain tissue and required delicate handling to prevent separation of the tumor mass during brain extraction.

Sampled tumor volumes produced by neuralized ESCs at 6 weeks post-transplantation were significantly larger (mean sample volume = 16.6 ± 1.3 mm^3; $p < 0.001$) than at 3 weeks post-transplantation (mean sample volume = 0.77 ± 0.12 mm^3; Figure 2B). Sampled tumor volumes produced by undifferentiated ESCs, taken three weeks after implantation had a mean sampled volume of 29.8 ± 3.5 mm^3 ($p < 0.001$; Figure 2B). The latter volume was significantly larger than sampled tumor volumes produced by neuralized ESCs, assessed at either 3 weeks or 6 weeks post-transplantation.

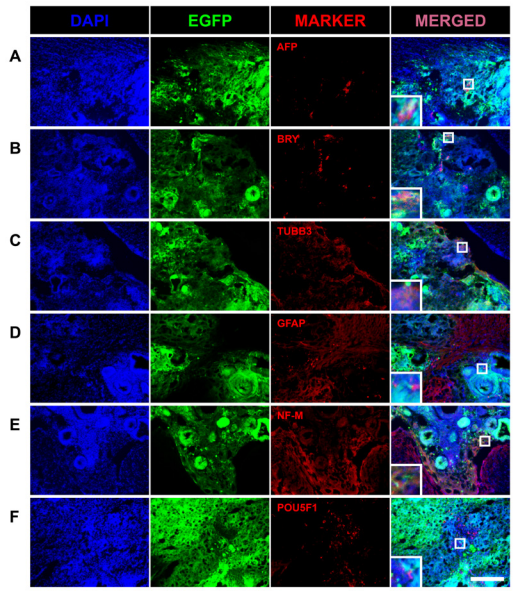

Figure 6
Brains Removed 3 Weeks After Transplantation of Neuralized B6 ESCs Into Syngeneic C57BL/6 Mice Contained Teratomas With Cells That Express Markers for the Three Primary Germ Layers as Well as for Mature Glia and Neurons and Pluripotent Stem Cells

(A-C) Frozen sections of tumors display markers for endoderm (AFP, **A**), mesoderm (BRY, **B**), and ectoderm (TUBB3, **C**). **(D)** Sections expressed GFAP more strongly in non-tumor areas; however, GFAP was expressed by some cells within the tumor. **(E)** NF-M was strongly expressed in adjacent areas but was also found in the tumor. **(F)** The pluripotent stem cell transcription factor POU5F1was

expressed within the tumor. In all panels, EGFP expression (green) indicates donor B6 cells. Cellular nuclei were stained with DAPI (blue). All images were taken from 10 µm thick frozen sections, and the scale bar in F (MERGED, large panel) equals 250 µm and applies to all large panels. Inserts in the merged panels are taken from the regions indicated by the small white boxes, enlarged an additional 4x. Note the co-expression of the specified markers and EGFP.

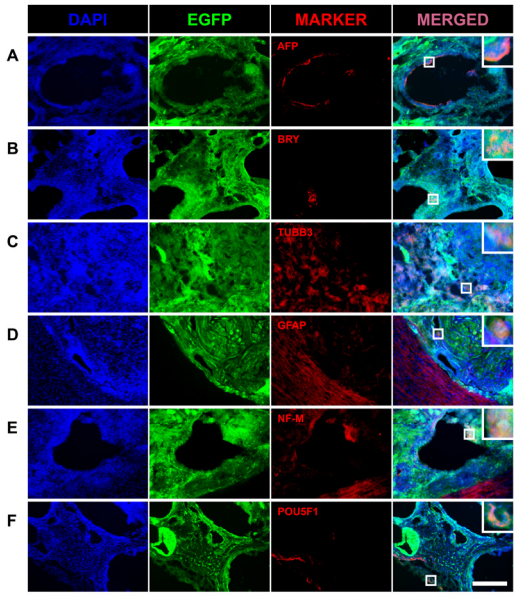

Figure 7
Teratomas Formed by Undifferentiated B6 ESCs 3 Weeks After Transplantation Into Syngeneic C57BL/6 Mice Expressed Markers for the Three Primary Embryonic Germ Layers as Well as For Mature Neurons and Glia and Pluripotent Stem Cells

(A-C) Sections of displayed markers for endoderm (AFP, **A**), mesoderm (BRY, **B**), and ectoderm (TUBB3, **C**). These teratomas expressed mature neuronal and glial markers to a lesser degree than the surrounding endogenous neural tissue. **(D)** Sections showed strong GFAP expression in adjacent brain parenchyma, and GFAP was expressed within the tumor. **(E)** Similarly, expression of NF-M was observed in tumor and non-tumor areas. **(F)** The pluripotency transcription factor POU5F1 was found within EGFP-labeled tissue. In all panels, EGFP expression (green) indicates donor B6 cells. Nuclei were stained with DAPI (blue), and all images were taken from 10 µm thick frozen sections. The scale bar in F (MERGED, large panel) equals 250 µm and applies to all large panels. Inserts are 4x additional magnification of the region indicated by the small white box in the merged panels.

Based on their histological and immunocytochemical features including cells that expressed markers for all the three primary embryonic germ layers, tumors produced by undifferentiated and neuralized B6 ESCs were teratomas (Figures 6, 7, & 8). Expression of markers for the three embryonic germ layers was shown by labeling for AFP, BRY and TUBB3in all treatment groups. Neurofilament-M and GFAP were also detected in all tumors; however, expression of the latter markers was not as extensive as their expression in adjacent brain parenchyma. The teratomas also expressed POU5F1/ OCT3/4 (Figures 6, 7, & 8).

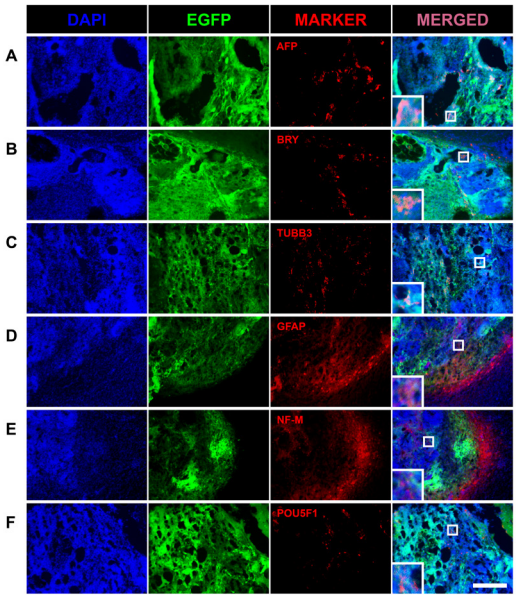

Figure 8
Tumors Formed by Neurally-Induced B6 ESCs at 6 Weeks Post-Transplantation (C57BL/6 Hosts) **Expressed Markers From the Three Primary Germ Layers as Well as Mature Glia and Neurons and Pluripotent Stem Cells**

(A-C) Sections of 6 week tumor growths displayed markers for endoderm (AFP, **A**), mesoderm (BRY, **B**), and ectoderm (TUBB3, **C**). **(D)** Sections expressed GFAP more strongly in non-tumor areas; however, many cells within the tumor expressed GFAP. **(E)** Coronal sections similarly expressed NF-M more strongly in non-tumor areas. **(F)** Labeling of sections revealed cells expressing the pluripotency marker POU5F1. In all panels, EGFP expression (green) indicates donor B6 cells. Nuclei were stained with DAPI (blue), all images were taken from 10 µm thick frozen sections. The scale bar in F (MERGED, large panel) equals 250 µm and applies to all large panels. Inserts are 4x additional magnification of the region indicated by the small white boxes.

3. DISCUSSION

3.1 ESC Growth Properties in Vitro

Our results indicate that undifferentiated, adherent B6 ESCs grow slowly and consistently produce small, irregularly shaped colonies when compared to undifferentiated B5 ESCs cultured under equivalent conditions. B6 Day 4 and Day 8 EBs formed after neural induction were also significantly smaller than those produced by B5 ESCs. Embryoid bodies from B5 cells on Day 4 were twice the size of B6 EBs at the same time point and achieved a size similar to B6 Day 8 EBs. These findings are in line with previous reports that C57BL/6-derived ESCs exhibited slower growth when compared to 129-derived ESCs (Ware, et al., 2003; Keskintepe, et al., 2007). A gene expression profile comparing a 129-derived ESC cell line (IMT11) with a C57BL/6 cell line (SMHBl6) showed upregulation of Ki-67 in IMT11 cells (Mansergh, et al., 2009). Since Ki-67 is a cell proliferation marker,

this upregulation suggests a higher growth rate for 129-derived ESCs and indicates differential growth rates between C57BL/6 and 129-derived ESC cell lines.

The irregular colony borders found among low density B6 ESC colonies could be due to premature differentiation, as this morphology is indicative of cellular differentiation at the edges of ESC colonies (Limaye et al., 2009). The B6 ESCs plated at a high density produced colonies with significantly larger diameters than those plated at the lower density, and colonies plated at higher density exhibited smoother borders with fewer irregularities. This density-dependent growth is consistent with other studies suggesting that mouse ESCs plated at higher densities experience a decrease in cell death and an increase in colony-forming efficiency (Mittal & Voldman, 2011). Embryonic stem cells may be releasing growth-promoting autocrine and paracrine factors that regulate cellular differentiation. For instance, one recently identified ESC autocrine factor is cycophilin A, a nonmitogenic survival-enhancing factor that influences mouse ESC growth and is also overexpressed in several cancers (Mittal & Voldman, 2011).

3.2 B6 Embryoid Bodies Form Neural Rosette-Like Structures

Four days after LIF removal, B6 EBs express markers for early ectoderm, mesoderm, and endoderm, and for pluripotent stem cells. This expression pattern is typical of Day 4 EBs from B5, B6 and other ESC lines (Mansergh et al., 2009; Bazou et al., 2011; Carpenedo, Sargent, & McDevitt, 2007). After induction, the B5 and B6 EBs contain large areas of cells expressing the neural precursor marker, nestin. The EBs also have significant numbers of cells expressing TUBB3, GFAP, and NF-M, indicating that they contain both immature neurons and maturing neuronal and glial cells. These findings are consistent with other reports that EBs at the end of the 4–/4+ RA induction protocol contain a heterozygous population of cells at different stages of neural differentiation (Meyer et al., 2004; Liu et al., 2000;).

By Day 8 of induction, the B6 EBs resembled neural rosettes with a specialized core of cells surrounded by layers of cells expressing markers for immature as well as mature neural cells (Zhang et al., 2001; Ueno et al., 2006). Neural rosettes can be derived by neural induction of murine, bovine, and primate (including human) ESCs or from neural plate tissue (Elkabetz et al., 2008; Lazzari et al., 2006; Perrier et al., 2004). Rosette neural stem cells are thought to be an intermediate between ESCs and true neural stem cells (Elkabetz et al., 2008). They display unique markers including promyelocytic leukemia zinc finger, a protein expressed in the neural plate, in addition to displaying markers from both undifferentiated embryonic and neural stem cells (Elkabetz et al., 2008; Chambers et al., 2009). Typically, rosette neural stem cells can be obtained after neural induction and attachment to an adherent surface (Germain, Banda, & Grabel, 2010).

One potential explanation for neural rosette-like formation by B6 ESCs is that EBs are recapitulating the inside-out pattern seen in the development of the vertebrate cortex (Van Ooyen, 2011). In cortical development, precursor cells are generated in the subventricular zone, and then divide asymmetrically to form more mature neural cells, after which they migrate along radial glia to the cortical plate (Frisen, Johansson, Lothian, & Lendahl, 1998; Zubler & Douglas, 2009). The oldest neurons are found closest to the ventricular zone, younger neurons migrate beyond previously formed layers to mature into more peripheral layers, and astrocyte development occurs near the ventricular zone (Germain et al., 2010). The Day 8 B6 EBs exhibit a central core of immature and mature neural cells as well as GFAP expressing cells. Glial fibrillary acidic protein and TUBB3 expressing cells extend from the EB center to the periphery, while cells expressing NF-M are less prominent in peripheral regions. Large numbers of TUBB3 expressing immature neurons are seen in both the core and periphery, with a much greater disbursement in the periphery than that of cells expressing the mature neuronal marker. The rosette-like structures formed by B6 EBs resemble an early stage of the recently reported cerebral organoids derived *in vitro* from pluripotent stem cells, including human ESCs and iPSCs exposed to retinoic acid as part of the induction protocol (Lancaster et al., 2013).

3.3 Mouse ESC Neural Induction Protocols

Many induction protocols and embryonic stem cell lines have been used to produce cells of a neural lineage, as manipulation of ESC signaling molecules and exposure of ESCs to different media can drive them to a variety of neural fates. For example, BLC 6 ESCs (derived from 129/SvJ) can be induced to generate neuronal cells with post-mitotic nerve cell characteristics using a modified 4–/4+ protocol in which EBs are plated on Day 4 of induction (Strubing et al., 1995), while these same ESCs can also produce neural cells when treated with NGF (Wobus, Grosse, & Schoneich, 1988). R1 ESCs derived from a 129S1 × 129X1 cross can be grown in adherent monoculture in the presence of RA to produce neural cells without EB formation (Xu et al., 2011). R1 ESCs, along with J1 (129S4/SvJae), D3 (129/SvJ), and CJ7 (129S1/SvImJ) ESCs can be aggregated and cultured in suspension for 4 days, reattached as EBs, and conditioned with medium supplemented with insulin, transferrin, selenium, and fibronectin (ITSFn) to produce neurons and glial cells (Okabe et al., 1996). D3 ESCs can be used in a 4–/4+ induction with the addition of either RA or icaritin on Day 4 of induction to produce neural rosettes, cholinergic neurons, and neuroglia cells (icaritin is a phytomolecule isolated from a herb that exhibits estrogen-like neuroprotective effects) (Wang et al., 2009). R1,

E14.1 (129/Ola), and B5 ESCs can be used in a five-stage induction protocol involving EB formation and plating, culture in ITSFn, subsequent culture in N2 medium containing bFGF/laminin, and withdrawal of bFGF to produce dopaminergic and serotonergic neurons (Lee et al., 2000). R1 ESCs can also be induced through a modified serum-free EB culture protocol to form neural rosettes, which have been hypothesized to be an intermediate state between ESCs and neural stem cells (NSCs) (Elkabetz et al., 2008).

Retinoic acid is an important signaling factor that regulates CNS development and the addition of RA during neural induction of ESCs drives them towards a neural fate and the production of specialized neurons and glia (Wang et al., 2009; Meyer et al., 2004; Bain et al., 1995; Pierret et al., 2010; Liu et al., 2000; Xu et al., 2011; Engberg et al., 2010). In addition, B5 ESCs can be induced to make NSC niche-like structures *in vitro* after using the 4–/4+ RA protocol and subsequent plating at high density on an entactin-collagen-laminin coated surface (Pierret et al., 2010). After the addition of RA to B6 Day 4 EBs, POU5F1, BRY, and AFP levels decrease significantly and are no longer expressed in Day 8 EBs (Figures 4 & 5; Table 1; Meyer et al., 2004; Okabe et al., 1996; Bain et al., 1995; Meyer et al., 2006; Pierret et al., 2007; Xu et al., 2011; Faherty et al., 2005; Meyer et al., 2009; Nonaka et al., 2008; Okada, Shimazaki, Sobue, & Okano, 2004). Using the 4–/4+ neuralization protocol, Liu et al. (2000) showed that the genetically modified 129Sv ESC line, ROSA26, produces more glial-like cells than neuronal cells; conversely, Meyer et al. (2004) demonstrated that B5 ESCs produce more neuronal-like cells when exposed to the same protocol. Using this neural induction protocol, the current study shows that B6 ESCs produce EBs containing similar percentages of cells expressing neuronal and glial markers.

3.4 Neuralized B6 EBs Produce Teratomas in Syngeneic C57BL/6 Mice

Neurally-induced B6 ESCs were transplanted into the left striatum of syngeneic C57BL/6 mice to assess their integration potential and to test their suitability for future experiments involving transplantation into mouse models of neurodegenerative disease, such as Parkinson's Disease. The implanted B6 ESCs formed tumors as assessed at 3 and 6 weeks post-transplantation. These tumors were teratomas that contained cells expressing markers for the three primary embryonic germ layers (Shao et al., 2007). As a positive control for teratoma formation (Yamanaka et al., 2008; Thomson et al., 1998; Pera, 2010), undifferentiated B6 ESCs were transplanted into the same brain region, and these grafts grew teratomas at such a rapid rate that all of the animals were sacrificed at an early time point.

One potential explanation for the development of teratomas in recipients of the neuralized ESCs is that undifferentiated ESCs may persist in the Day 8 B6 EBs. The 4–/4+ RA neural induction protocol produces a heterogeneous cell population within the Day 8 EBs, containing approximately 40% NSCs (i.e., cells expressing nestin) along with other cell types at various stages of neural differentiation (Cai & Grabel, 2007). If some transplanted cells remain in an undifferentiated pluripotent state, they likely have tumorigenic potential (Brederlau et al., 2006). Since as little as two undifferentiated ESCs can form a teratoma (Lawrenz et al., 2004), it is possible that some undifferentiated ESCs were transplanted, even though POU5F1 expressing cells were not observed in the Day 8 EBs used for transplantations. Forced expression of POU5F1 expression in either mouse or human NSCs is sufficient to induce them into a pluripotent state (Kim et al., 2009; Kim et al., 2009), and while less likely, teratomas in our studies may have formed due to mutations in the implanted, neuralized ESCs.

Some cells within all tumors tested in the current study expressed POU5F1, while POU5F1 expression was not observed in Day 8 B6 EBs. It is possible that neuralized, transplanted ESCs again expressed POU5F1; however, POU5F1expression in the teratomas is consistent with neural progenitor cells exhibiting tumorigenic potential. Finally, epigenetic changes in NSCs appear to induce pluripotency and teratoma formation (Lee et al., 2011) and could have played a role in reprogramming the fate of the transplanted cells.

CONCLUSION

B6 ESCs consistently grew slower than B5 ESCs when gown as adherent, undifferentiated cells or as EBs during neural induction. While the 4–/4+ RA induction protocol is sufficient to commit B5 ESCs to a neural fate, the neuralization effect on B6 ESCs appears less complete. The slower growth rate of B6 ESCs may also contribute to a less complete neural induction. When either undifferentiated or neuralized B6 ESCs were transplanted into the left striatum of syngeneic mice, teratomas were produced from the donor cells. Tumor growth was more rapid in mice receiving undifferentiated ESCs. Teratomas formed from undifferentiated ESCs achieved volumes at 3 weeks post-transplantation that were significantly greater than the volumes of teratomas formed at 6 weeks from neuralized ESCs. This suggests that after neural induction, ESCs had differentiated primarily into neural progenitors, immature neural cells and mature neural cells. This conclusion is consistent with the expression of mature neural marker expression in the Day 8 B6 EB as well as the derivation within these EBs of structures resembling that of neural rosettes. Modification of the

RA induction protocol (such as earlier or more prolonged exposure to RA) may reduce the formation of teratomas after injection of the neuralized cells into syngeneic brains and could influence the formation of neural rosette rosettes within the EBs. Other neural induction protocols, such as those that produce substrate-adherent ESC cell-derived neural aggregates or direct reprogramming of B6 ESCs may provide more complete and/or selective neural fate specification.

ACKNOWLEDGEMENTS

The authors thank Drs. Jason Meyer and Greg Tullis for providing constructive comments on the initial manuscript. Funding for this study was provided by a grant from the University of Missouri Research Board to MDK. CLD was supported by a teaching assistantship provided by the Division of Biological Sciences, University of Missouri.

REFERENCES

Abe, K., Niwa, H., Iwase, K., Takiguchi, M., Mori, M., Abé, S. I., …, Yamamura, K. I. (1996). Endoderm-specific gene expression in embryonic stem cells differentiated to embryoid bodies. *Exp. Cell Res.*, *229*, 27-34. doi: 10.1006/excr.1996.0340

Alison, M. R., & Islam, S. (2009). Attributes of adult stem cells. *J. Pathol*, *217*, 144-160. doi: 10.1002/path.2498

Auerbach, W., Dunmore, J. H., Fairchild-Huntress, V., Fang, Q., Auerbach, A. B., Huszar, D., & Joyner, A. L. (2000). Establishment and chimera analysis of 129/SvEv- and C57BL/6-derived mouse embryonic stem cell lines. *Bio. Techniques*, *29*, 1024-1028, 1030, 1032.

Bain, G., Kitchens, D., Yao, M., Huettner, J. E., & Gottlieb, D. I. (1995). Embryonic stem cells express neuronal properties in vitro. *Dev. Biol.*, *168*, 342-357. doi: 10.1006/dbio.1995.1085

Bazou, D., Kearney, R., Mansergh, F., Bourdon, C., Farrar, J., & Wride, M. (2011). Gene expression analysis of mouse embryonic stem cells following levitation in an ultrasound standing wave trap. *Ultrasound Med. Biol.*, *37*, 321-330. doi: 10.1016/j.ultrasmedbio.2010.10.019

Bibel, M., Richter, J., Schrenk, K., Tucker, K. L., Staiger, V., Korte, M, …, Barde, Y. A. (2004). Differentiation of mouse embryonic stem cells into a defined neuronal lineage. *Nat. Neurosci*., *7*, 1003-1009. doi: 10.1038/nn1301

Bjorklund, L. M., Sanchez-Pernaute, R., Chung, S., Andersson, T., Chen, I. Y., McNaught, K. S., …, Isacson, O. (2002). Embryonic stem cells develop into functional dopaminergic neurons after transplantation in a Parkinson rat model. *Proc. Natl. Acad. Sci. USA*, *99*, 2344-2349. doi: 10.1073/pnas.062039699

Brederlau, A., Correia, A. S., Anisimov, S. V., Elmi, M., Paul, G., Roybon, L., …, Li, J. Y. (2006). Transplantation of human embryonic stem cell-derived cells to a rat model of Parkinson's disease: effect of in vitro differentiation on graft survival and teratoma formation. *Stem Cells*, *24*, 1433-1440. doi: 10.1634/stemcells.2005-0393

Brook, F. A., & Gardner, R. L. (1997). The origin and efficient derivation of embryonic stem cells in the mouse. *Proceedings of the National Academy of Sciences of the United States of America*, *94*, 5709-5712. doi: 10.1073/pnas.94.11.5709

Bryant, C. D., Zhang, N. N., Sokoloff, G., Fanselow, M. S., Ennes, H. S., Palmer, A. A., & McRoberts, J. A. (2008). Behavioral differences among C57BL/6 substrains: Implications for transgenic and knockout studies. *J. Neurogenet*, 22, 315-331. doi: 10.1080/01677060802357388

Cai, C., & Grabel, L. (2007). Directing the differentiation of embryonic stem cells to neural stem cells. *Dev. Dyn.*, *236*, 3255-3266. doi: 10.1002/dvdy.21306

Carpenedo, R. L., Sargent, C. Y., & McDevitt, T. C. (2007). Rotary suspension culture enhances the efficiency, yield, and homogeneity of embryoid body differentiation. *Stem Cells*, *25*, 2224-2234. doi: 10.1634/stemcells.2006-0523

Chambers, S. M., Fasano, C. A., Papapetrou, E. P., Tomishima, M., Sadelain, M., & Studer, L. (2009). Highly efficient neural conversion of human ES and iPS cells by dual inhibition of SMAD signaling. *Nat. Biotechnol.*, *27*, 275-280. doi: 10.1038/nbt.1529

Chen, X. J., Kovacevic, N., Lobaugh, N. J., Sled, J. G., Henkelman, R. M., & Henderson, J. T. (2006). Neuroanatomical differences between mouse strains as shown by high-resolution 3D MRI. *Neuroimage*, *29*, 99-105. doi: 10.1016/j.neuroimage.2005.07.008

Cheng, J., Dutra, A., Takesono, A., Garrett-Beal, L., & Schwartzberg, P. L. (2004). Improved generation of C57BL/6J mouse embryonic stem cells in a defined serum-free media. *Genesis*, *39*, 100-104. doi: 10.1002/gene.20031

Collins, F. S., Rossant, J., & Wurst, W. (2007). A mouse for all reasons. *Cell*, *128*, 9-13. doi: 10.1016/j.cell.2006.12.018

Cook, M. N., Bolivar, V. J., McFadyen, M. P., & Flaherty, L. (2002). Behavioral differences among 129 substrains: implications for knockout and transgenic mice. *Behav. Neurosci.*, *116*, 600-611. doi: 10.1037//0735-7044.116.4.600

Crusio, W. E., Schwegler, H., & Van Abeelen, J. H. (1991). Behavioural and neuroanatomical divergence between two sublines of C57BL/6J inbred mice. *Behavioural Brain Research*, *42*, 93-97. doi: 10.1016/S0166-4328(05)80043-9

Eisenberg, L. M., & Eisenberg, C. A. (2003). Stem cell plasticity, cell fusion, and transdifferentiation. *Birth Defects Res C Embryo Today*, *69*, 209-218. doi: 10.1002/bdrc.10017

Elkabetz, Y., Panagiotakos, G., Al Shamy, G., Socci, N. D., Tabar, V., & Studer, L. (2008). Human ES cell-derived neural rosettes reveal a functionally distinct early neural stem cell stage. *Genes Dev.*, *22*, 152-165. doi: 10.1101/gad.1616208

Engberg, N., Kahn, M., Petersen, D. R., Hansson, M., & Serup, P. (2010). Retinoic acid synthesis promotes development of neural progenitors from mouse embryonic stem cells by suppressing endogenous, Wnt-dependent nodal signaling. *Stem Cells*, *28*, 1498-1509. doi: 10.1002/stem.479

Faherty, S., Kane, M. T., & Quinlan, L. R. (2005). Self-renewal and differentiation of mouse embryonic stem cells as measured by Oct 4 gene expression: effects of lif, serum-free medium, retinoic acid, and dbcAMP. *In Vitro Cell Dev. Biol. Anim.*, *41*, 356-363. doi: 10.1290/0412078.1

Frisen, J., Johansson, C. B., Lothian, C., & Lendahl, U. (1998). Central nervous system stem cells in the embryo and adult. *Cell Mol. Life Sci.*, *54*, 935-945.

Germain, N., Banda, E., & Grabel, L. (2010). Embryonic stem cell neurogenesis and neural specification. *J. Cell Biochem.*, *111*, 535-542. doi: 10.1002/jcb.22747

Gertsenstein, M., Nutter, L. M., Reid, T., Pereira, M., Stanford, W. L., Rossant, J., & Nagy, A. (2010). Efficient generation of germ line transmitting chimeras from C57BL/6N ES cells by aggregation with outbred host embryos. *PLoS One 5*, e11260. doi: 10.1371/journal.pone.0011260

Hughes, E. D., Qu, Y. Y., Genik, S. J., Lyons, R. H., Pacheco, C. D., Lieberman, A. P., & Saunders, T. L. (2007). Genetic variation in C57BL/6 ES cell lines and genetic instability in the Bruce4 C57BL/6 ES cell line. *Mammalian Genome: Official Journal of the International Mammalian Genome Society*, *18*, 549-558. doi: 10.1007/s00335-007-9054-0

Katsetos, C. D., Del Valle, L., Geddes, J. F., Assimakopoulou, M., Legido, A., Boyd J. C., ..., Khalili, K. (2001). Aberrant localization of the neuronal class III beta-tubulin in astrocytomas. *Archives of Pathology & Laboratory Medicine*, *125*, 613-624. doi:10.1043/0003-9985(2001)125<0613:ALOTNC>2.0.CO;2

Kawase, E., Suemori, H., Takahashi, N., Okazaki, K., Hashimoto, K., & Nakatsuji, N. (1994). Strain difference in establishment of mouse embryonic stem (ES) cell lines. *The International Journal of Developmental Biology*, *38*, 385-390.

Keskintepe, L., Norris, K., Pacholczyk, G., Dederscheck, S. M., & Eroglu, A. (2007). Derivation and comparison of C57BL/6 embryonic stem cells to a widely used 129 embryonic stem cell line. *Transgenic Research*, *16*, 751-758. doi: 10.1007/s11248-007-9125-8

Kim, J. B., Greber, B., Arauzo-Bravo, M. J., Meyer, J., Park, K. I., Zaehres, H., & Schöler, H. R. (2009). Direct reprogramming of human neural stem cells by OCT4. *Nature*, *461*, 649-643. doi :10.1038/nature08436

Kim, J. B., Sebastiano, V., Wu, G., Arauzo-Bravo, M. J., Sasse, P., Gentile, L., ..., Schöler, H. R. (2009). Oct4-induced pluripotency in adult neural stem cells. *Cell*, *136*, 411-419. doi: 10.1016/j.cell.2009.01.023.

Kispert, A., & Herrmann, B. G. (1994). Immunohistochemical analysis of the Brachyury protein in wild-type and mutant mouse embryos. *Dev. Biol.*, *161*, 179-193. doi: 10.1006/dbio.1994.1019

Kleinsmith, L. J., & Pierce, G. B. Jr. (1964). Multipotentiality of single embryonal carcinoma cells. *Cancer Res.*, *24*, 1544-1551.

Lancaster, M. A., Renner, M., Martin, C. A., Wenzel, D., Bicknell, L. S., Hurles, M. E., ..., Knoblich, J. A. (2013). Cerebral organoids model human brain development and microcephaly. *Nature*, 501, 373-379. doi: 10.1038/nature12517

Lawrenz, B., Schiller, H., Willbold, E., Ruediger, M., Muhs, A., & Esser, S. (2004). Highly sensitive biosafety model for stem-cell-derived grafts. *Cytotherapy*, *6*, 212-222. doi:10.1080/14653240410006031

Lazzari, G., Colleoni, S., Giannelli, S. G., Brunetti, D., Colombo, E., Lagutina, I., , Broccoli, V. (2006). Direct derivation of neural rosettes from cloned bovine blastocysts: a model of early neurulation events and neural crest specification in vitro. *Stem Cells*, *24*, 2514-2521. doi: 10.1634/stemcells.2006-0149

Ledermann, B. (2000). Embryonic stem cells and gene targeting. *Experimental Physiology*, *85*, 603-613.

Ledermann, B., & Burki, K. (1991). Establishment of a germ-line competent C57BL/6 embryonic stem cell line. *Experimental Cell Research*, *197*, 254-258. doi: 10.1016/0014-4827(91)90430-3

Lee, S. H., Appleby, V., Jeyapalan, J. N., Palmer, R. D., Nicholson, J. C., Sottile, V, ..., Scotting, P. J. (2011). Variable methylation of the imprinted gene, SNRPN, supports a relationship between intracranial germ cell tumours and neural stem cells. J. *Neurooncol*, *101*, 419-428. doi: 10.1007/s11060-010-0275-9

Lee, S. H., Lumelsky, N., Studer, L., Auerbach, J. M., & McKay, R. D. (2000). Efficient generation of midbrain and hindbrain neurons from mouse embryonic stem cells. *Nature Biotechnology*, *18*, 675-679. doi :10.1038/76536

Li, Y., & Tanaka, T. (2011). Self-renewal, pluripotency and tumorigenesis in pluripotent stem cells revisited. In C. S. Atwood (Ed.), *Embryonic stem cells—recent advances in pluripotent stem cell-based regenerative medicine: InTech* (pp.339-358). doi: 10.5772/15196

Limaye, A., Hall, B., & Kulkarni, A. B. (2009). Manipulation of mouse embryonic stem cells for knockout mouse production. *Current Protocols in Cell Biology*, *19*(13), 11-24. doi: 10.1002/0471143030.cb1913s44

Liu, S., Qu, Y., Stewart, T. J., Howard, M. J., Chakrabortty, S., Holekamp, T. F., & McDonald, J. W. (2000). Embryonic stem cells differentiate into oligodendrocytes and myelinate in culture and after spinal cord transplantation. *Proc. Natl. Acad. Sci. USA*, *97*, 6126-6131. doi: 10.1073/pnas.97.11.6126

Mansergh, F. C., Daly, C. S., Hurley, A. L., Wride, M. A., Hunter, S. M., & Evans, M. J. (2009). Gene expression profiles during early differentiation of mouse embryonic stem cells. *BMC Dev. Biol.*, *9*, 5. doi: 10.1186/1471-213X-9-5

Martin, G. R. (1981). Isolation of a pluripotent cell line from early mouse embryos cultured in medium conditioned by teratocarcinoma stem cells. *Proceedings of the National Academy of Sciences of the United States of America*, *78*, 7634-7638. doi: 10.1073/pnas.78.12.7634

Meyer, J. S., Katz, M. L., Maruniak, J. A., & Kirk, M. D. (2004). Neural differentiation of mouse embryonic stem cells in vitro and after transplantation into eyes of mutant mice with rapid retinal degeneration. *Brain Res.*, *1014*, 131-144. doi: 10.1016/j.brainres.2004.04.019

Meyer, J. S., Katz, M. L., Maruniak, J. A., & Kirk, M. D. (2006). Embryonic stem cell-derived neural progenitors incorporate into degenerating retina and enhance survival of host photoreceptors. *Stem Cells*, *24*, 274-283. doi: 10.1634/stemcells.2005-0059

Meyer, J. S., Tullis, G., Pierret, C., Spears, K. M., Morrison, J. A., & Kirk, M. D. (2009). Detection of calcium transients in embryonic stem cells and their differentiated progeny. *Cell Mol. Neurobiol*, *29*, 1191-1203. doi: 10.1007/s10571-009-9413-3

Mitalipov, S., & Wolf, D. (2009). Totipotency, pluripotency and nuclear reprogramming. In U. Martin (Ed.), *Engineering of stem cells* (pp.185-199). Berlin: Springer-Verlag Berlin. doi: 10.1007/10_2008_45

Mittal, N., & Voldman, J. (2011). Nonmitogenic survival-enhancing autocrine factors including cyclophilin A contribute to density-dependent mouse embryonic stem cell growth. *Stem Cell Res.*, *6*, 168-176. doi: 10.1016/j.scr.2010.10.001

Nichols, J., Zevnik, B., Anastassiadis, K., Niwa, H., Klewe-Nebenius, D., Chambers I, ..., Smith, A. (1998). Formation of pluripotent stem cells in the mammalian embryo depends on the POU transcription factor Oct4. *Cell*, *95*, 379-391. doi: 10.1016/S0092-8674(00)81769-9

Nonaka, J., Yoshikawa, M., Ouji, Y., Matsuda, R., Nishimura, F., Yamada, S., …, Sakaki, T. (2008). CoCl(2) inhibits neural differentiation of retinoic acid-treated embryoid bodies. *J. Biosci. Bioeng.*, *106*, 141-147. doi: 10.1263/jbb.106.141

Okabe, S., Forsberg-Nilsson, K., Spiro, A. C., Segal, M., & McKay, R. D. (1996). Development of neuronal precursor cells and functional postmitotic neurons from embryonic stem cells in vitro. *Mechanisms of Development*, *59*, 89-102. doi: 10.1016/0925-4773(96)00572-2

Okada, Y., Shimazaki, T., Sobue, G., & Okano, H. (2004). Retinoic-acid-concentration-dependent acquisition of neural cell identity during in vitro differentiation of mouse embryonic stem cells. *Dev. Biol.*, *275*, 124-142. doi: 10.1016/j.ydbio.2004.07.038

Okita, K., Ichisaka, T., & Yamanaka, S. (2007). Generation of germline-competent induced pluripotent stem cells. *Nature*, *448*, 313-317. doi: 10.1038/nature05934

Pera, M. F. (2010). Defining pluripotency. *Nat. Methods*, *7*, 885-887.

Perrier, A. L., Tabar, V., Barberi, T., Rubio, M. E., Bruses, J., Topf, N., …, Studer, L. (2004). Derivation of midbrain dopamine neurons from human embryonic stem cells. *Proc. Natl. Acad. Sci. USA*, *101*, 12543-12548. doi: 10.1073/pnas.0404700101

Pierret, C., Morrison, J. A., Rath, P., Zigler, R. E., Engel, L. A, Fairchild, C. L., …, Kirk, M. D. (2010). Developmental cues and persistent neurogenic potential within an in vitro neural niche. *BMC Dev. Biol.*, *10*, 5. doi: 10.1186/1471-213X-10-5

Pierret, C., Spears, K., Morrison, J. A., Maruniak, J. A., Katz, M. L., & Kirk, M. D. (2007). Elements of a neural stem cell niche derived from embryonic stem cells. *Stem Cells Dev.*, *16*, 1017-1026. doi: 10.1089/scd.2007.0012

Seong, E., Saunders, T. L., Stewart, C. L., & Burmeister, M. (2004). To knockout in 129 or in C57BL/6: that is the question. *Trends in Genetics*, *20*, 59-62. doi: 10.1016/j.tig.2003.12.006

Shao, H., Wei, Z., Wang, L., Wen, L., Duan, B., Manga, L., & Boua, S. (2007). Generation and characterization of mouse parthenogenetic embryonic stem cells containing genomes from non-growing and fully grown oocytes. *Cell Biology International*, *31*, 1336-1344. doi: 10.1016/j.cellbi.2007.05.008

Solter, D. (2006). From teratocarcinomas to embryonic stem cells and beyond: A history of embryonic stem cell research. *Nat. Rev. Genet.*, *7*, 319-327. doi: 10.1038/nrg1827

Spears, K. (2011). *Immunogenic properties of neuralized embryonic stem cells in a model of allogeneic intracranial transplantation*. Columbia, MO: University of Missouri.

Srivastava, A. S., Malhotra, R., Sharp, J., & Berggren, T. (2008). Potentials of ES cell therapy in neurodegenerative diseases. *Curr. Pharm. Des.*, *14*, 3873-3879.

Stevens, L. C., & Little, C. C. (1954). Spontaneous testicular teratomas in an inbred strain of mice. *Proc. Natl. Acad. Sci. USA*, *40*, 1080-1087. doi: 10.1073/pnas.40.11.1080

Strubing, C., Ahnert-Hilger, G., Shan, J., Wiedenmann, B., Hescheler, J., & Wobus, A. M. (1995). Differentiation of pluripotent embryonic stem cells into the neuronal lineage in vitro gives rise to mature inhibitory and excitatory neurons. *Mechanisms of Development*, 53, 275-287. doi: 10.1016/0925-4773(95)00446-8

Tabibnia, G., Cooke, B. M., & Breedlove, S. M. (1999). Sex difference and laterality in the volume of mouse dentate gyrus granule cell layer. *Brain Research*, *827*, 41-45. doi: 10.1016/S0006-8993(99)01262-7

Takahashi, K., & Yamanaka, S. (2006). Induction of pluripotent stem cells from mouse embryonic and adult fibroblast cultures by defined factors. *Cell*, *126*, 663-676. doi: 10.1016/j.cell.2006.07.024

Takahashi, K., Tanabe, K., Ohnuki, M., Narita, M., Ichisaka T, Tomoda, K., & Yamanaka, S. (2007). Induction of pluripotent stem cells from adult human fibroblasts by defined factors. *Cell*, *131*, 861-872. doi: 10.1016/j.cell.2007.11.019

Thomson, J. A., Itskovitz-Eldor, J., Shapiro, S. S., Waknitz, M. A., Swiergiel, J. J., Marshall, V. S., & Jones, J. M. (1998). Embryonic stem cell lines derived from human blastocysts. *Science*, *282*, 1145-1147. doi: 10.1126/science.282.5391.1145

Ueno, M., Matsumura, M., Watanabe, K., Nakamura, T., Osakada, F., Takahashi, M, …, Sasai, Y. (2006). Neural conversion of ES cells by an inductive activity on human amniotic membrane matrix. *Proc. Natl. Acad. Sci. USA*, *103*, 9554-9559. doi: 10.1073/pnas.0600104103

Van Ooyen, A. (2011). Using theoretical models to analyse neural development. *Nat. Rev. Neurosci.*, *12*, 311-326. doi :10.1038/nrn3076

Wahlsten, D., Metten, P., & Crabbe, J. C. (2003). Survey of 21 inbred mouse strains in two laboratories reveals that BTBR T/+ tf/tf has severely reduced hippocampal commissure and absent corpus callosum. *Brain Research*, *971*, 47-54. doi: 10.1016/S0006-8993(03)02354-0

Walker, A. S., Goings, G. E., Kim, Y., Miller, R. J., Chenn, A., & Szele, F. G. (2010). Nestin reporter transgene labels multiple central nervous system precursor cells. *Neural Plast.*, *2010*, 894374.

Wang, Z., Wang, H., Wu, J., Zhu, D., Zhang, X., Ou, L., …, Lou, Y. (2009). Enhanced co-expression of beta-tubulin III and choline acetyltransferase in neurons from mouse embryonic stem cells promoted by icaritin in an estrogen receptor-independent manner. *Chem. Biol. Interact.*, *179*, 375-385.

Ware, C. B., Siverts, L. A., Nelson, A. M., Morton, J. F., & Ladiges, W. C. (2003). Utility of a C57BL/6 ES line versus 129 ES lines for targeted mutations in mice. *Transgenic Research*, *12*, 743-746.

Wobus, A. M., Grosse, R., & Schoneich, J. (1988). Specific effects of nerve growth factor on the differentiation pattern of mouse embryonic stem cells in vitro. *Biomedica Biochimica Acta*, 47, 965-973.

Xu, H., Fan, X., Wu, X., Tang, J., & Yang, H. (2005). Neural precursor cells differentiated from mouse embryonic stem cells relieve symptomatic motor behavior in a rat model of Parkinson's disease. *Biochem. Biophys. Res. Commun.*, *326*, 115-122.

Xu, J., Wang, H., Liang, T., Cai, X., Rao, X., Huang, Z., & Sheng, G. (2011). Retinoic acid promotes neural conversion of mouse embryonic stem cells in adherent monoculture. *Mol. Biol. Rep.*.

Yamanaka, S., Li, J., Kania, G., Elliott, S., Wersto, R. P., Eyk, J. V., …, Boheler, K. R. (2008). Pluripotency of embryonic stem cells. *Cell and Tissue Research*, *331*, 5-22.

Zhang, S. C., Wernig, M., Duncan, I. D., Brustle, O., & Thomson, J. A. (2001). In vitro differentiation of transplantable neural precursors from human embryonic stem cells. *Nat. Biotechnol*, *19*, 1129-1133.

Zubler, F., & Douglas, R. (2009). A framework for modeling the growth and development of neurons and networks. *Front Comput. Neurosci.*, *3*, 25.

